proposed earlier whereby cobaltinitrite was reduced to Co^{2+}, and the nitrite was oxidized to free nitrate when the samples were left standing. In light of the complexity of the results obtained from the ligand exchange reaction involving the thiocyanate anion, care must be exercised in its interpreation, and further work is warranted to clarify the chemistry.

Finally, Juranič[40] reported that ^{59}Co NMR chemical shifts were sensitive to the ring size of chelating ligands, and we found evidence that ^{59}Co NMR chemical shifts were also highly sensitive to the stereochemical arrangement of chelating ligands during the course of this work. These findings will be reported in a future publication.

Acknowledgment. R. J. Buist is grateful to the Natural Sciences and Engineering Research Council of Canada for financial support.

Registry No. Co, 7440-48-4.

(39) Sasaki, T.; Susuki, K. Z.; Matsumoto, A.; Saito, K. *Inorg. Chem.* **1982**, *21*, 1825.
(40) Juranič, N.; Čelap, M. B.; Vučelič, D.; Malinar, M. J.; Radivojša, P. N. *J. Coord. Chem.* **1979**, *9*, 117.
(41) Figgis, B. N. *Introduction to Ligand Fields*; Interscience Publishers: 1966; p 231.

Oxirenes and Ketocarbenes from α-Diazoketone Photolysis: Experiments in Rare Gas Matrices. Relative Stabilities and Isomerization Barriers from MNDOC-BWEN Calculations

Christian Bachmann,[1] Thomas Yao N'Guessan,[1] Fabrice Debû,[2] Maurice Monnier,[2] Jean Pourcin,[2] Jean-Pierre Aycard,[2] and Hubert Bodot*[,2]

Contribution from Département de Chimie, Université Nationale de Côte d'Ivoire, 22 BP 582, Abidjan 22, Côte d'Ivoire, and Laboratoire de Physique des Interactions Ioniques et Moléculaires, URA CNRS 773, Université de Provence, Centre de Saint-Jérôme, Case 542, 13397 Marseille Cedex 13, France. *Received March 6, 1990. Revised Manuscript Received May 22, 1990*

Abstract: Matrix-isolated α-diazoketones (DZ) $RCOCN_2R$ (R = CH_3 or CD_3) were photolyzed and their reactions were monitored by FT-IR spectroscopy. The ketene (KE) products from the Wolff rearrangement were always more abundant than the α,β-unsaturated ketones (ON); this selectivity increased when a broad band source (λ > 230 nm) was used instead of a monochromatic laser source (457.9 nm). Oxirenes (OX) were detected as minor, but well-identified reaction products, stable at temperatures less than 25 K, even under the monochromatic irradiation; they isomerized to KE when irradiated at λ > 230 nm. With matrices doped with carbon monoxide, the reaction diverted toward ketoketene, which certainly resulted from ketocarbene (KC) trapped by CO molecules. The kinetic data showed that the rate constants of DZ → KC, KC → KE, KC → ON, and KC → OX processes have the same order of magnitude. After complete DZ photolysis, the KE concentration still increased under extended irradiation; therefore, $KC(T_0)$ is suspected to be another reaction product that slowly photoisomerized to KE. Some IR absorption bands might correspond to that intermediate, but unambiguous assignments could not be made. On the other hand, our previous oxirene identification has been supported by ab initio calculations at the SCF level, which justified the high-frequency value of oxirene ν(C=C). To account for the results of matrix isolation experiments and for those previously recorded during the gas-phase photolysis of several DZ [R = CH_3, $(CH_3)_3C$; R-R = $-(CH_2)_4-$], the relative stabilities of different isomers (KC, OX, and KE) were computed, and the assumed reaction paths from KC to reaction products were studied, in each series, through the MNDOC semiempirical method. Substituent effects and ring strain deeply influence the oxirene stability. Considering that the photolysis and photoisomerization processes occur on the singlet potential energy surface, we finally established a unified energy diagram, approximately scaled, that gathers together the different species in different electronic states and allows the interpretation of the main reaction features.

Since the initial publications,[3] a number of studies have dealt with the Wolff rearrangement (WR). Usually, the initial step consists of a photoinduced decomposition of an α-diazoketone (Scheme I). The ketocarbenes (KC), mainly obtained in photochemical conditions, are now currently observed and identified in ESR experiments (triplet state)[4-9] and through IR and UV-visible spectroscopies.[9] These studies, and our own results about the gas-phase photolysis of α-diazoketones,[10] have ruled out the hypothesis of a concerted mechanism proposed by Kaplan et al.[11,12]

Chart I

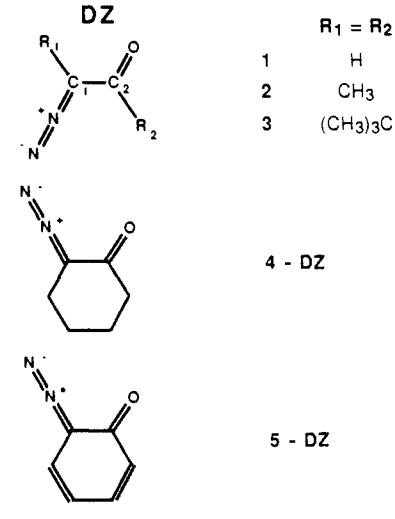

(1) Université Nationale de Côte d'Ivoire.
(2) Université de Provence.
(3) Wolff, L. *Justus Liebigs Ann. Chem.* **1912**, *394*, 23-36, and references therein.
(4) (a) Murai, H.; Safarik, I.; Torres, M.; Strausz, O. P. *J. Am. Chem. Soc.* **1988**, *110*, 1025-1032. (b) Murai, H.; Ribo, J.; Torres, M.; Strausz, O. P. *J. Am. Chem. Soc.* **1981**, *103*, 6422-6426.
(5) Tomioka, H.; Okuno, H.; Izawa, Y. *J. Org. Chem.* **1980**, *45*, 5278-5283.
(6) Torres, M.; Raghunathan, P.; Bourdelande, J. L.; Clement, A.; Toth, G.; Strausz, O. P. *Chem. Phys. Lett.* **1986**, *127*, 205-209.
(7) Moriconi, E. J.; Murray, J. J. *J. Org. Chem.* **1964**, *29*, 3577-3584.
(8) Murai, H.; Torres, M.; Ribo, J.; Strausz, O. P. *Chem. Phys. Lett.* **1983**, *101*, 202-205.
(9) (a) Hayes, R. A.; Hess, T. C.; McMahon, R. J.; Chapman, O. L. *J. Am. Chem. Soc.* **1983**, *105*, 7786-7787. (b) McMahon, R. J.; Chapman, O. L.; Hayes, R. A.; Hess, T. C.; Krimmer, H. P. *J. Am. Chem. Soc.* **1985**, *107*, 7597-7606.

0002-7863/90/1512-7488$02.50/0

Table I. First-Order Analysis[a] of 2-DZ and 2-DZ-d_6 Photolysis[b] Performed in Krypton Matrices[c]

	$(\nu_i - \nu_j)$[d]	ID[e]	$k \times 10^5$, s^{-1}	A_0, cm^{-1}	A_∞, cm^{-1}
2-DZ (λ = 457.9, T_D = 20 K)	2082.0–2041.8	DZ	10.5 ± 0.4	0.66 ± 0.01	(5 ± 8) × 10^{-3}
	1671.0–1656.0	DZ	9.8 ± 0.4	0.49 ± 0.01	(0 ± 6) × 10^{-3}
	1305.0–1293.0	DZ	10.6 ± 0.6	0.063 ± 0.001	(1 ± 1) × 10^{-3}
	2131.0–2120.5	KE	6.3 ± 0.9	(0 ± 2) × 10^{-3}	0.039 ± 0.002
	1722.0–1718.0	ON-s$Z\alpha$	3.2 ± 0.4	(−3 ± 1) × 10^{-3}	0.033 ± 0.002
	1718.0–1713.0	ON-s$Z\beta$	10.1 ± 1.3	(−4 ± 1) × 10^{-3}	0.014 ± 0.001
	1700.0–1689.0	ON-s-*E*	2.4 ± 1.0	(14 ± 8) × 10^{-3}	0.058 ± 0.009
	2140.0–2131.0	OX	5.9 ± 2.0	(0 ± 2) × 10^{-3}	0.015 ± 0.002
2-DZ-d_6 (λ = 457.9, T_D = 12 K)	2093.0–2030.0	DZ	9.2 ± 0.5	2.45 ± 0.04	0.13 ± 0.04
	2123.0–2110.0	KE	5.4 ± 0.3	(−4 ± 4) × 10^{-3}	0.23 ± 0.01
	1712.0–1707.0	ON-s$Z\alpha$	2.2 ± 0.1	(−2 ± 2) × 10^{-3}	0.111 ± 0.003
	1707.0–1702.0	ON-s$Z\beta$	6.9 ± 0.7	(−1 ± 2) × 10^{-3}	0.053 ± 0.002
	2135.0–2130.0	OX	3.6 ± 0.2	(−1 ± 6) × 10^{-3}	0.078 ± 0.002
2-DZ-d_6 (λ > 230, T_D = 12 K)	2111.0–2020.0	DZ	121 ± 8	1.25 ± 0.09	−0.1 ± 0.1
	2130.0–2104.0	KE	60 ± 10	(0 ± 1) × 10^{-1}	1.43 ± 0.12
	1714.0–1700.0	ON-s-*Z*	40 ± 8	(0 ± 2) × 10^{-2}	0.19 ± 0.02
	1701.0–1689.0	ON-s-*E*	38 ± 14	(0 ± 4) × 10^{-2}	0.15 ± 0.04
2-DZ-d_6[f] (λ = 457.9, T_D = 20 K)	1662.5–1630.0	DZ	7.4 ± 0.4	1.27 ± 0.02	0.13 ± 0.02
	1683.0–1670.0	KK[g]	6.3 ± 0.1	(8 ± 8) × 10^{-3}	0.16 ± 0.01

[a] A_0 and A_∞ are the optimized integrated intensities at zero and infinite time, respectively. [b] Irradiation wavelengths λ in nanometers. [c] M/S = 2000. [d] ν_i and ν_j are the frequency limits used to calculate the integrated intensities of absorption bands (see Experimental Section). [e] ID, identification of the compound that corresponds to the absorption band. [f] Matrix: Kr/CO/solute = 2000/100/1. [g] KK = ketoketene $CD_3COC(CD_3)$=C=O.

Scheme I

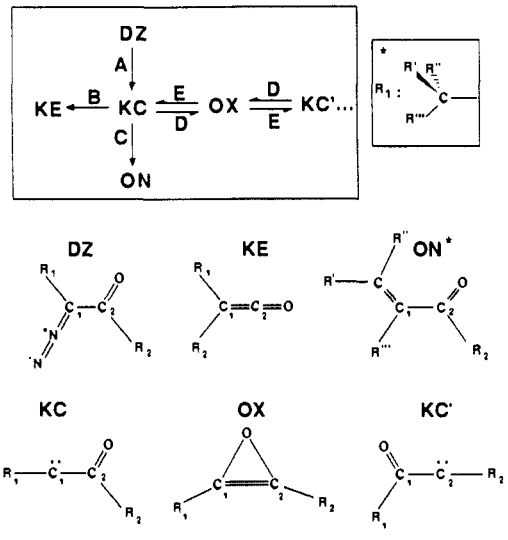

and according to which the R_2 shift would be concomitant with the loss of nitrogen.

Concurrently with the formation of a ketene (KE) or WR product (Scheme I, path **B**), the ketocarbene leads to α,β-unsaturated ketones (ON) (Scheme I, path C), subsequently reported as being the concurrent reaction since the α,β-unsaturated ketones, as the ketenes, are usually obtained.

Moreover, the KC isomerization via an oxirene species (KC ⇌ OX ⇌ KC') has been suggested (Scheme I, paths D and E).[13-15] This latter reaction has been evidenced through experimental studies on α-diazoketones having isotopic carbon label[13,14] or different R_1 and R_2 substituents.[15]

Recently, we reported the photolysis experiments of 3-diazo-2-butanone (**2**-DZ) isolated in rare gas matrices and monitored by FT-IR spectroscopy, which provide direct observation of oxirene (R_1 = R_2 = CH_3 or CD_3) vibrational absorption bands.[16] The thermal isomerization of this oxirene to the corresponding ketene has been observed at 25 K, suggesting an activation process of ~2 kcal/mol (Scheme I, path E).

Previously, we studied the photolysis of **2**-DZ and two other α-diazoketones in the gas phase[10] (Chart I). The main results concern the following: (1) The increasing amount of ketene (**2**-KE) produced from photolysis of **2**-DZ when collisions with argon atoms occur suggests that the α,β-unsaturated ketone originates from high vibrational levels of the ketocarbene. (2) The photolysis of **3**-DZ leads to a large amount of ketene **3**-KE, in disagreement with the hypothesis of a concerted mechanism proposed according to Kaplan,[12] which photolyzed **3**-DZ in solution.

In the present study, we report photolysis experiments on **2**-DZ and **2**-DZ(d_6) isolated in rare gas matrices. The amounts of the reaction products are carefully examined, including the oxirenes and ketocarbenes that would be expected as short-lived species under other experimental conditions. In addition, kinetic data were available from FT-IR monitoring.

The theoretical studies concerning the WR were essentially limited to the simplest system **1** (R_1 = R_2 = H).[17-24] For that system, a number of interesting potential energy surface (PES) features have been obtained (e.g., the isomerization activation energy of the oxirene has been estimated at ~2 kcal/mol). However, these studies were generally restricted to singlet PES, the triplet PES studies being sparse.[19,21,25,26] EHT calculations

(10) (a) Marfisi, C.; Verlaque, P.; Davidovics, G.; Pourcin, J.; Pizzala, L.; Aycard, J. P.; Bodot, H. *J. Org. Chem.* **1983**, *48*, 533–537. (b) Marfisi, C. Thèse de Spécialité, Université de Provence, Marseille, 1981.
(11) Kaplan, F.; Meloy, G. K. *J. Am. Chem. Soc.* **1966**, *88*, 950–956.
(12) Kaplan, F.; Mitchell, M. L. *Tetrahedron Lett.* **1979**, 759–762.
(13) (a) Czismadia, I. G.; Front, J.; Strausz, O. P. *J. Am. Chem. Soc.* **1968**, *90*, 7360–7361. (b) Thornton, D. E.; Gosavi, R. K.; Strausz, O. P. *J. Am. Chem. Soc.* **1970**, *92*, 1768–1769. (c) Frater, G.; Strausz, O. P. *J. Am. Chem. Soc.* **1970**, *92*, 6654–6656.
(14) (a) Zeller, K. P.; Meier, H.; Kolshorn, H.; Muller, E. *Chem. Ber.* **1972**, *105*, 1875–1886. (b) Zeller, K. P. *Tetrahedron Lett.* **1977**, 707–708.
(15) Matlin, S. A.; Sammes, P. G. *J. Chem. Soc., Perkin Trans. 1* **1972**, 2623–2630.
(16) (a) Debū, F.; Monnier, M.; Verlaque, P.: Davidovics, G.; Pourcin, J.; Bodot, H.; Aycard, J. P. *C. R. Acad. Sci.* Paris, *Ser. 2* **1986**, *303*, 897–902. (b) Debū, F. Thèse de Spécialité, Université de Provence, Marseille, 1986.
(17) Czismadia, I. G.; Gunning, H. E.; Gosavi, R. K.; Strausz, O. P. *J. Am. Chem. Soc.* **1973**, *95*, 133–137.
(18) Strausz, O. P.: Gosavi, R. K.: Denes, A. S.; Czismadia, I. G. *J. Am. Chem. Soc.* **1976**, *98*, 4784–4786.
(19) (a) Tanaka, K.; Yoshimine, M. *J. Am. Chem. Soc.* **1980**, *102*, 7655–7662. (b) Bargon, J.: Tanaka, K.; Yoshimine, M. *Computational Methods in Chemistry*: Bargon, J., Ed.: Plenum Press: New York, 1979; pp 239–274.
(20) Bouma, W. J.; Nobes, R. H.; Radom, L.; Woodward, C. E. *J. Org. Chem.* **1982**, *47*, 1869–1875.
(21) Novoa, J. J.; McDouall, J. J. W.; Robb, M. A. *J. Chem. Soc., Faraday Trans. 2* **1987**, *83*, 1629–1636.
(22) Schröder, S.: Thiel, W. *J. Am. Chem. Soc.* **1985**, *107*, 4422–4430.
(23) Schröder, S.: Thiel, W. *J. Am. Chem. Soc.* **1986**, *108*, 7985–7989.
(24) Schröder, S.: Thiel, W. *J. Mol. Struct. (THEOCHEM)* **1986**, *31*, 141–150.

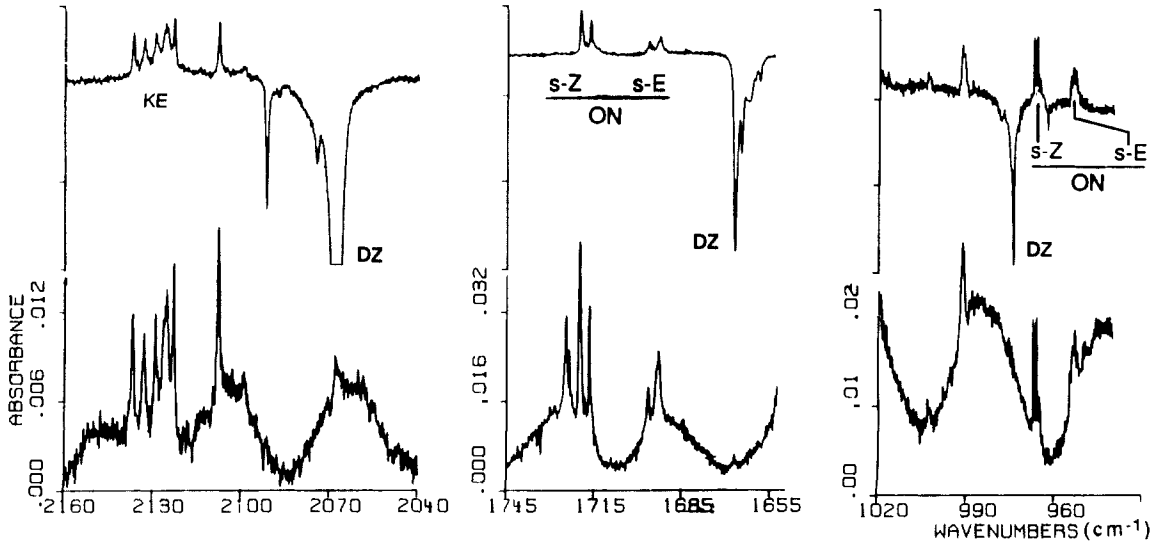

Figure 1. FT-IR spectrum of the reaction products issued from krypton matrix isolated 3-diazo-2-butanone (**2**-DZ) photolysis after 1140 min of irradiation at the 457.9-nm Ar^+ laser line (power 140 mW). Matrix/solute M/S = 2000; deposition temperature T_D = 20 K. The upper part is the difference spectrum with respect to that recorded before irradiation.

concerning the $CH_3\ddot{C}C(O)H$ and $CH_3\ddot{C}C(O)CH_3$ systems have also been published;[17] in each case, they predict an unstable oxirene species. The factors expected to govern the oxirene stabilities were not emphasized in these studies; in particular, the question of substituent effects needs clarification. Moreover, a lack of information remains about the CH_3 and $(CH_3)_3C$ shifts involved in a number of WR experiments, the ring contractions occurring with cyclic α-diazoketones and the related concurrent reactions.

In order to allow a better understanding of our previous experimental results (in rare gas matrices and in the gas phase), a theoretical study was required. Thus, the oxirene and ketocarbene relative stabilities, the corresponding interconversion activation barriers, and the relative energies of the transition states related to the WR and to its concurrent reactions were estimated[27] for **2**, **3**, and **4** derivatives.

Finally, all these results, collected together with some electronic transition energies, lead us to suggest a whole energy diagram including all the isomerization reactions involved.

Photolysis of 3-Diazo-2-butanone and Its Deuterated Isotopomer in Rare Gas Matrices

As the photolysis experiments have been monitored by FT-IR spectroscopy, the vibrational spectra of these α-diazoketones have been carefully studied in a previous paper.[28] Such a preliminary investigation was necessary to look for the possibilities to discriminate the conformer spectra. Force field calculations have shown the closeness of s-*E* and gauche (due to the OCCN dihedral angle estimated at 30°) vibrational frequencies, which precludes from distinguishing between conformational and sites effects.

Expecting different kinetic behaviors of the two conformers during photolysis, we have carefully controlled the decay of the main absorption bands. As any clear deviations from first-order process have been observed (Table I), we must conclude that either the rate constants are equal or that one of the conformers, presumably the s-*E* one[17,29] predominates.

Important information had been previously collected by Strausz et al.[13] from the photolysis of matrix-isolated **2**-DZ [^{13}C]carbonyl isotopomer: the WR product, **2**-KE, was formed with 30% scrambling (partial formation of $(CH_3)_2{}^*C{=}C{=}O$). The authors concluded that the reaction occurs through a 70% oxirene pathway. Therefore, isolation of **2**-OX was a challenge that required the control of reaction products at every stage of photolysis. Moreover, a selective irradiation might avoid the oxirene photoisomerization. As reported before,[16] we succeeded in getting and identifying the IR spectra of **2**-OX and in observing its thermal isomerization at 25 K as well as its photoisomerization. Further details are reported here.

First, we must consider the major reaction products. The difference spectrum shown on Figure 1 corresponds to the monochromatic irradiation (Ar^+ laser working at 457.9 nm) of **2**-DZ and gives, as positive absorption bands, those of **2**-KE (2133–2099 cm^{-1}), the multiplet being assigned to site effects, and those of **2**-ON, conformer s-*Z* (1720.0 and 1716.9; 966.3 and 965.5 cm^{-1}) and conformer s-*E* (1696.8 and 1693.0; 954.1, 953.2, and 952.9 cm^{-1}) as identified from direct matrix isolation experiments on **2**-ON and subsequent s-*E* → s-*Z* UV photoisomerization in krypton matrix (see Experimental Section). The negative signals of the difference spectrum are those of **2**-DZ, which has been photolyzed.

When matrix-isolated **2**-DZ underwent a broad-band irradiation (filtered high-pressure Hg lamp, λ > 230 nm), it decomposed in a few minutes and gave the same major products with the same IR absorption bands, but an increased selectivity was observed when the **2**-KE/**2**-ON-s-*Z* ratio was estimated from the absorption band integrated intensities [2140–2094 cm^{-1} for ν(C=C=O) of **2**-KE and 1722–1713 cm^{-1} for ν(C=O) of **2**-ON-s-*Z*], we got 10.3 and 1.8 for broad-band and monochromatic irradiations, respectively. When the same experiments were performed on **2**-DZ-d_6 in krypton matrix, the corresponding ratios were 8.6 and 3.6. In the gas phase,[10] the similar mole ratio (**2**-KE/**2**-ON) was 4.3 regardless of the irradiation mode, the subsequent photolysis of **2**-KE being taken into account. Whereas this last result agrees with the classical scheme of fast $S_n \rightarrow S_1$ processes for **2**-DZ and/or **2**-KC, a different scheme must be proposed for experiments performed in rare gas matrices.

For **2**-ON and **2**-ON-d_6 as reaction products, the ratios of integrated intensities of carbonyl stretching absorption bands were $2 \leq (s\text{-}Z/s\text{-}E) \leq 38$, opposite to the one observed for direct matrix isolation ($s\text{-}Z/s\text{-}E \leq 1$). As this last value corresponded to

(25) Baird, N. C.; Taylor, K. F. *J. Am. Chem. Soc.* **1978**, *100*, 1333–1338.
(26) Kim, K. S.; Schaefer, H. F., III *J. Am. Chem. Soc.* **1980**, *102*, 5390–5392.
(27) The species

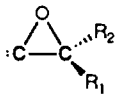

and $R_1C{\equiv}COR_2$ are possibly stable isomers of the ketocarbene, as evidenced by theoretical studies on the **1** system.[19,20,22] However, these calculations revealed high-energy barriers from the ketocarbene. Consequently, these species were not considered in the present study.
(28) Davidovics, G.; Debū, F.; Marfisi, C.; Monnier, M.; Aycard, J. P.; Pourcin, J.; Bodot, H. *J. Mol. Struct.* **1986**, *147*, 29–45.
(29) Sorriso, S. *Z. Naturforsch.* **1979**, *34B*, 1530–1534.

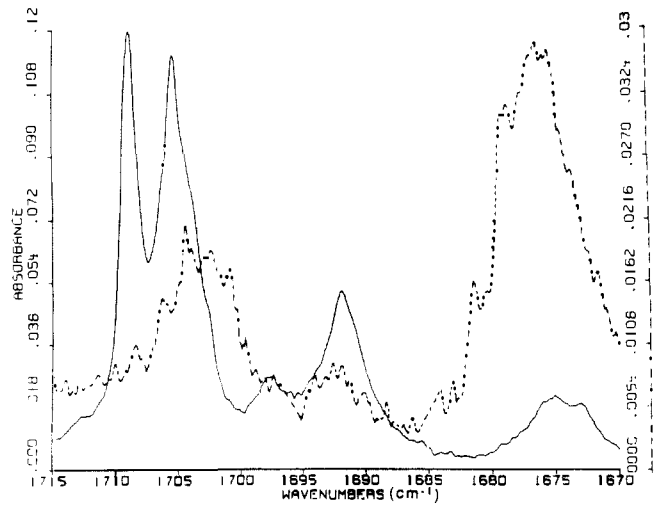

Figure 2. FT-IR spectra of some reaction products CD_3—CO—CD=CD_2 and CD_3—CO—C(CD_3)=C=O issued from deuterated 3-diazo-2-butanone (**2**-DZ-d_6) photolysis. Irradiations at λ = 457.9 nm. CO-doped krypton matrices: Kr/CO/solute = 500/5/1 (T_D = 12 K) (—) and 2000/100/1 (T_D = 20 K) (---).

room-temperature equilibrium, owing to sudden molecular freeze, the photochemical pathway to α,β-unsaturated ketones turned out to be stereoselective. The low temperature precluded thermal stereoisomerization, and shorter irradiation times from any photochemical rotamerization as those observed after long UV irradiation[30] (see Experimental Section). Therefore, the observed stereoselectivity may be a priori attributed to conformational features of the ketocarbene precursor and/or to cage effects. In the future, site structure modelings such as the one performed for matrix-embedded 2-fluoroethanol[31] will be useful to go further in the discussion.

When krypton matrices were doped with carbon monoxide, the photolysis of **2**-DZ-d_6 was partly (1% CO) or largely (5% CO) diverted to the benefit of a new product, the deuterated methyl acetyl ketene $CH_3COC(CH_3)$=C=O produced from the reaction of **2**-KC-d_6 with a CO molecule and identified from its ν(C=O) absorption band at 1676 cm^{-1} as in similar molecules[9,32] (Figure 2). Other IR absorption bands clearly belonged to this new compound: 2106, 1300.6, 1284.6, and 1280.6 cm^{-1}. As the ν(C=C=O) stretching frequency of this ketoketene (KK) must lie in the 2150–2100-cm^{-1} range,[32] we can assign the 2106-cm^{-1} band to that vibrational mode. The strong absorption of carbon monoxide at 2135 cm^{-1} presumably hid other components of a multiplet, the 2106-cm^{-1} band of which would be at the lowest frequency side. Moreover, these experiments showed a decrease of **2**-KE-d_6 and **2**-ON-d_6 yields: as an example, the integrated intensities of the **2**-ON-d_6-s-*Z* ν(C=O) absorption band (1712–1702 cm^{-1}) were 5 and 0.3 times that of the ketoketene (1680–1668 cm^{-1}) after photolysis in 1% CO and 5% CO krypton matrices, respectively. Therefore, it may be argued that the CO molecules, being in the vicinity of the **2**-KC-d_6 molecules, caught these species at the expense of the usual major photolysis products. Actually, for the 5% CO krypton matrix, one CO molecule at least was present among the 20 nearest neighbors of the matrix-isolated species.

FT-IR spectra have been systematically recorded at different times during the photolysis process. As the integrated intensities of numerous absorption bands were plotted against time, we have been able to detect minor reaction products that had kinetic behaviors different from that of major products. When **2**-DZ-d_6 was photolyzed (irradiation at λ > 230 nm) in a xenon matrix

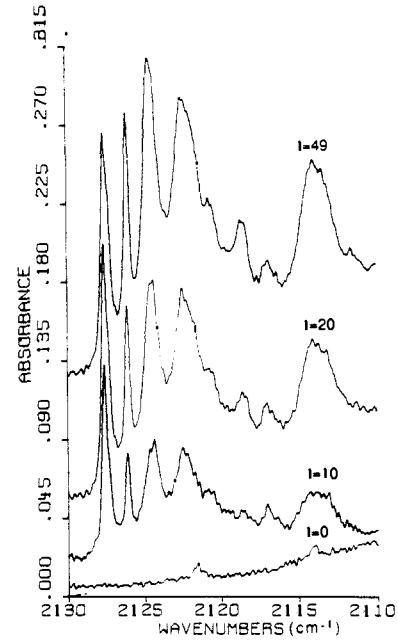

Figure 3. FT-IR spectra of some reaction products OX and KE issued from xenon matrix isolated deuterated 3-diazo-2-butanone (**2**-DZ-d_6) photolysis (filtered high-pressure Hg lamp λ > 230 nm) at different irradiation times (in minutes). M/S = 2000; T_D = 20 K.

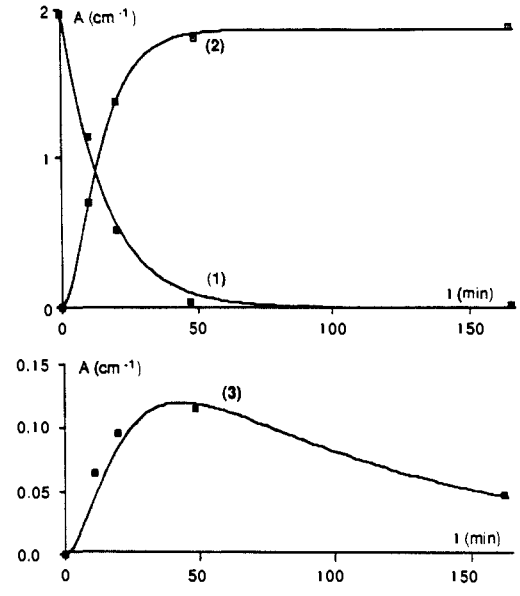

Figure 4. Integrated intensities (*A* in reciprocal centimeters) of different absorption bands at different reaction times (in minutes) during photolysis (λ > 230 nm) of **2**-DZ-d_6 isolated in a xenon matrix (M/S = 2000; T_D = 20 K). (1) 2097.0–2040.0 cm^{-1} (DZ); (2) 2138.0–2097.0 cm^{-1} (KE + OX); (3) 2128.7.0–2125.7 cm^{-1} (OX); beyond 165 min *A* (cm^{-1}) 0.037 (270 min); 0.001 (1170 min).

[matrix/solute (M/S) = 2000], the absorption band at 2127.6 cm^{-1} was easily distinguishable from the other components of the multiplet (2130–2110 cm^{-1}); it was the most intense peak after 10 min (Figure 3); its integrated intensity reached a maximum value between 20 and 40 min and then decreased and disappeared after 1000 min (Figure 4 and Figure 1 in ref 16a). With some other absorption bands that had the same behavior, the 2127.6-cm^{-1} band was assigned[16] to **2**-OX-d_6. In the early stage of the reaction, this oxirene appeared as an efficient competitor to ketene and α,β-unsaturated ketone, but in its turn, it photoisomerized during extended irradiation. After 150 min, **2**-DZ-d_6 was fully photolyzed, but **2**-KE-d_6 concentration still increased to a slight extent, whereas **2**-ON-d_6 concentration did not change at all. These observations suggested that OX + $h\nu$ → KE was the main process of this secondary reaction; it was not observed during the

(30) Krantz, A.; Goldfarb, T. D.; Lin, C. Y. *J. Am. Chem. Soc.* **1972**, *94*, 4022–4024.
(31) Charbonnier, S.; Viani, R.; Pourcin, J.; Bodot, H. *J. Mol. Struct.* **1987**, *161*, 265–281.
(32) (a) Wentrup, C.; Gross, G.; Berstermann, H. M.; Lorencak, P. *J. Org. Chem.* **1985**, *50*, 2877–2881. (b) Clemens, R. J.; Witzeman, J. S. *J. Am. Chem. Soc.* **1989**, *111*, 2186–2193.

monochromatic irradiation at 457.9 nm.

The kinetic analysis of different photolysis experiments has been performed assuming a first-order behavior for DZ, KE, and ON integrated intensities against time; these intensities were supposed to follow the Beer–Lambert law. Some of the results (k, A_0, and A_∞) are reported in the Experimental Section (Table I). It appears that the KE and ON rate constants are significantly lower than the corresponding DZ decay rate constant; these observations are compatible with a kinetic scheme involving a reaction intermediate (X) from which the different reaction products are afforded: DZ $\rightarrow$ X (k_1); KE $\leftarrow$ X $\rightarrow$ ON (k_2 and k_3). The X $\rightarrow$ OX pathway has also to be considered. Experimental values are $k(\mathrm{KE}) \approx k(\mathrm{ON})$. $k(\mathrm{DZ})$ is larger than these values, but never by more than 4 times. This means that k_1, k_2, and k_3 have the same order of magnitude; therefore, first-order analyses are no more rigorously valid, but they provide approximate rate constant values that are acceptable (no more than 10% gap) as has been shown through simulations.[16b] The kinetic analysis has been stopped at this step owing to limitations of experimental accuracies and to the reinforced complexity of the reaction scheme [X may be KC(S_1) and/or KC(T_0)]. In spite of these simplifications, we can draw some meaningful conclusions from the observations.

2-DZ and **2**-DZ-d_6 decay rate constants (Table I) do not differ more than 10% when the photolysis are performed, strictly under the same experimental conditions, at 457.9-nm irradiation. For the other rate constants (KE, ON, and OX), there are no significant deviations, therefore no important isotope effect. In spite of the low intensities of the **2**-OX absorption band (see A_∞ in Table I), we have been able to record its values and to analyze them as part of a first-order kinetic scheme. Actually, through these experiments, oxirenes appear as normal reaction products, and not as reaction intermediates. When irradiated at $\lambda > 230$ nm, **2**-DZ-d_6 photolyses faster (Table I), but the comparison between the irradiation powers is not straightforward. From the kinetic data reported on Figure 4 (xenon matrix), we have estimated the OX $\rightarrow$ KE photoisomerization rate constant to be $\sim 10^{-5}$ s^{-1}, which contrasts with the fast DZ decay ($\sim 90 \times 10^{-5}$ s^{-1}).

For the experiment performed in krypton matrix doped with 5% carbon monoxide (Figure 2), the DZ decay and the KK appearance are normal first-order processes and the rate constant difference does not exceed 15%; a rigorous equality would have opened the hypothesis of a KC/CO collapse faster than photolysis.

The last step, but not the least difficult procedure, requires estimations of reaction product proportions. As the molar absorption coefficients strongly vary from one compound to another, from one absorption band to another, it is necessary but difficult to get their values from experiments when the compound is not available as a stable species at room temperature. It is just the case with thermally unstable reaction intermediates such as oxirenes. But, as **2**-OX-d_6 exclusively isomerizes to **2**-KE-d_6, we just have to evaluate the **2**-KE-d_6 concentration increase, which exactly corresponds to the OX initial concentration. Other procedures have been used to estimate the yields of products (Table II) and are described in the Experimental Section.

When we make the assessments of photolysis products before complete evolution, the balance is short of 21% (457.9 nm) or 7% ($\lambda > 230$ nm), whereas longer irradiation times decrease these deficits. It may be concluded that some reaction product was not taken into account; **2**-KC(T_0) is a good candidate to be this missing product. Actually, it is thermally stable to 25 K and probably to higher temperatures, and it is able to slowly photoisomerize at 457.9 nm; triplet ketocarbenes are indeed known to absorb visible light.[9,33] Some IR absorption bands may be distinguished from that of other products (KE, ON, and OX). Their intensities are quite low, but they have exactly the same kinetic behavior with successive increase and decrease (change after 420 min) for the experiment reported in Table II (**2**-DZ-d_6 irradiated at 457.9 nm). The ratio of integrated intensities at two irradiation times [A(420)/A(1110)] is the same (1.7–1.8) for the three more intense bands of that group (see Experimental Section), in good agreement with that obtained from the balance (1.5). For different aromatic KC, the ν(C=O) vibrational bands have been located[9] between 1665 and 1679 cm^{-1}. Without any conjugation, **2**-KC-d_6 might exhibit a carbonyl absorption at higher frequency. The only absorption bands that may be attributed to that reaction intermediate are those located between 1687 and 1720 cm^{-1} and previously assigned to **2**-ON-d_6 (s-E and s-Z with site splittings). The **2**-KC-d_6 carbonyl band may probably coincide with one of the **2**-ON-d_6 absorption bands; if they really superimposed, it may be detected through kinetic analysis. Indeed, two different rate constants have been obtained for the two bands previously attributed to s-$Z\alpha$ and to s-$Z\beta$ (Table I); one of the two may have been disturbed by the **2**-KC-d_6 carbonyl band.

Table II. Product Yields after Photolysis of 3-Diazo-2-butanone (**2**-DZ) and Its Deuterated Isotopomer **2**-DZ-d_6

			product yield, %				
irradiation[a]	λ, nm	t, min	DZ	KE	ON	OX	(KC)[f]
2-DZ-d_6 (1)	457.9	420	22.2	28.5	23.5	5.0	20.8
		600	18.0	34.1	24.2	6.1	17.6
		1110	9.4	36.2	31.7	8.9	13.8
	>230	49	0.0	69.0	16.5	7.0	7.5
		49[b]	0.0	76.0	16.5	0.0	7.5
		1110	0.0	78.0	18.5	3.5	0.0[g]
		1110[c]	0.0	81.5	18.5	0.0	0.0
2-DZ (2)	457.9	80	0.0	75.0 +4.0[e]	19.0		
	<290	10	3.0[d]	49.5 +17.5[e]	18.4		

[a] (1) In krypton matrix (M/S = 2000); (2) in the gas phase.[10] [b] A 49-min irradiation + annealing (30 min at 25 K). [c] A 1110-min irradiation + annealing (20 min at 25 K). [d] With +11.6% $CH_3COCOCH_3$ owing to initial O_2 presence in the IR cell. [e] CH_2=$CHCH_3$ issued from KE photolysis. [f] Presumed identity. [g] **2**-KC photoisomerization is assumed to be completely achieved after such an irradiation time.

Theoretical Method

Several semiempirical methods are currently used to study systems containing up to 50 atoms from first and second rows. Indeed, some of these methods like MINDO/3,[34] MNDO,[35] and AM1[36] are known to provide reliable results (e.g., heats of formation, geometries), particularly when they are applied to ground states of stable molecules. Within the framework of these models, it is usually assumed that a significant part of the electron correlation is implicitly included through the parametrization, since this one is derived from experimental data. However, these data are essentially related to ground states of stable molecules; consequently, the resulting parametrizations are less suitable to study transition states. In particular, the reliability of the calculated activation barriers is questionable. Introducing an explicit electron correlation treatment within these models is a procedure that looks like an expedient and has to be used very carefully, since overestimated correlation energies might theoretically result.

For these reasons, the MNDOC method[37] seems very attractive since its parametrization is derived from experimental data by means of an explicit treatment of the electron correlation, through second-order perturbation theory using a Brillouin–Wigner expansion with Epstein–Nesbet energy denominators (BWEN). Therefore, the use of this same treatment in further calculations appears more suitable and is consistent within the method. Accordingly, the transition-state parameters, and hence the activation barriers, are expected to be more reliable when they are obtained from MNDOC calculations. Indeed, the MNDOC method has

(33) Sander, W.; Müller, W.; Sustmann, R. *Angew. Chem., Int. Ed. Engl.* **1988**, *27*, 572–574.

(34) Bingham, R. C.; Dewar, M. J. S.; Lo, D. H. *J. Am. Chem. Soc.* **1975**, *97*, 1285–1293.

(35) Dewar, M. J. S.; Thiel, W. *J. Am. Chem. Soc.* **1977**, *99*, 4899–4907.

(36) Dewar, M. J. S.; Zoebish, E. G.; Healy, E. F.; Stewart, J. J. P. *J. Am. Chem. Soc.* **1985**, *107*, 3202–3209.

(37) (a) Thiel, W. *J. Am. Chem. Soc.* **1981**, *103*, 1413–1420. (b) *Ibid.* 1420–1425. (c) Schweig, A.; Thiel, W. *J. Am. Chem. Soc.* **1981**, *103*, 1425–1431. (d) Thiel, W. *QCPE* **1982**, *No. 14*, 438.

been used to study ground singlet PES related to some systems such as **1**; the results were in good agreement with ab initio calculations including high level of electron correlation.[22-24]

We have used the MNDOC-BWEN method with standard parameters.[37] As noted by Thiel, such calculations provide estimates of correlation energy close (within 90–110%) to the corresponding values deduced from configuration interaction method including all the doubly excited configurations (DCI). Thus, it is possible to correct for size consistency by using the Langhoff–Davidson (LD) formula.[38] This latter approximation is discussed below.

As mentioned previously, several ketocarbenes have been identified, in their triplet state, from ESR experiments.[4-9] Moreover, some theoretical studies, although restricted to unsubstituted species **1**, concluded that the ground state of **1**-KC (formylmethylene, HC̈-CHO) is once again a triplet. At the ab initio level, the closed-shell S_1 lies higher than ground state T_0 by 17 and 25 kcal/mol according to Tanaka et al.[19] and Baird and Taylor,[25] respectively.[39] However, from ab initio calculations on reaction B (Scheme I) of species **1**, the activation barrier is relatively high on the triplet PES (58 kcal/mol), whereas it is almost zero on the first singlet PES.[19] In these circumstances, it is not surprising that an intersystem crossing process has been invoked in a number of WR studies.[4,8,9,21,40,41] Moreover, and according to Tanaka et al.,[19] it is noticeable that reaction D (Scheme I), which leads to the elusive oxirene, would be much more easy on the singlet PES than on the triplet one. Indeed, the activation barrier on the singlet PES for **1** is 5 kcal/mol while the triplet **1**-OX lies 47.3 kcal/mol higher than the triplet **1**-KC. The corresponding values from MC-SCF calculations[21] are 2.9 and 47.3 kcal/mol, respectively.

The hydrogen shift reaction $CH_3\ddot{C}H \rightarrow CH_2{=}CH_2$ has also been studied through ab initio methods including high level electron correlation. The activation energy related to its first triplet PES is more than 50 kcal/mol, while it is close to zero on the ground PES.[42,43] Thus, one can expect that reaction C (Scheme I) also occurs on the singlet surface. All these results convinced us of the usefulness of singlet surface calculations. In the present study, a large part of calculations are devoted to singlet PES.

In order to save computational time, the geometries were optimized at the SCF level (instead at the BWEN level). The resulting deviations on heats of formation are expected to be lower than 2 kcal/mol.[23] The transition states were localized by the reaction coordinate technique,[44] and all the geometrical parameters were optimized, unless otherwise specified, by employing the DFP algorithm.[45] Different reaction coordinates have been selected.[46] Some geometrical and symmetrical constraints have been imposed.

All fixed methyl groups (i.e., nonmigrating) were assumed with a 3-fold symmetry axis. Similarly, the carbon fragment of each fixed *tert*-butyl group was also assumed with a 3-fold symmetry axis. When there were several fixed CH_3 (reactions D and E for **2** and reactions B to E for **3**), they were kept identical with each other. In reaction B (**3**), all the parameters of the migrating *tert*-butyl group were relaxed except its CH_3 groups (with 3-fold symmetry axis), which remained identical with each other, but were different from that of the fixed *tert*-butyl group. In each reaction of the cyclohexanic series (**4**), the C–H distances were held equal to each other, except for the two hydrogen atoms of the CH_2 bound to the carbenoid carbon in reaction C. In each oxirene molecule, the two C–O bond lengths were held equal owing to $R_1 = R_2$. Accordingly, in KE molecules, $(C)_2C{=}C{=}O$ were assumed to have C_{2v} symmetry, except for **4**-KE where the C_1 carbon atom, included in a ring, slightly deviated from the plane defined by its three bound atoms.

Table III. Relative Energies from MNDOC-BWEN Calculations[a]

	relative energies, kcal/mol			
	KE	KC	OX	ON[c]
1	0.0[b]	65.2	76.7	
2	0.0	60.7	65.0	8.8[d]
3	0,0	50.2	46.2	−20.0[e]
4	0.0	66.3	104.9	5.5[f]

[a] Valucs including the LD correction; see text and ref 47. [b] Calculated heat of formation −11.7 kcal/mol; experimental value −11.4 kcal/mol.[48] [c] Lowest energy conformer; CC_1C_2O dihedral angles (dcg) in footnotes *d–f*. [d] 59.1. [e] 81.8. [f] 173.5.

Table IV. Activation Barriers[a] from MNDOC-BWEN Calculations[b]

	activation barrier, kcal/mol			
	KC → KE B	KC → ON C	KC → OX D	OX → KC E
1	2.4		17.3	5.8
2	12.7	23.0	11.6	7.3
3	23.3	24.6	9.4	13.5
4	10.9	20.0	38.6	0.0

[a] Processes B–E defined on Scheme 1. [b] See footnote *a* of Table III.

The relative energies of stable isomers deduced from heats of formation are reported in Table III. The values related to **1** are also indicated; though they were published earlier,[22] and in order to permit a more reliable comparison, we have once more performed these calculations but, in addition, we have corrected for size consistency by means of the LD formula.[47] The activation barriers corresponding to reactions B–E are reported in Table IV. A selection of the most important geometrical features are reported in Table V.

Finally, in order to clarify critical points concerning the identification of **2**-OX and the wavelength requirements of its photoisomerization, some ab initio calculations have been performed.[49]

(38) Langhoff, S. R.; Davidson, E. R. *Int. J. Quantum Chem.* **1974**, *8*, 61–65.

(39) The same gap was estimated at 23 kcal/mol through MNDO calculations; a corresponding value of 20 kcal/mol was derived for $CH_3\ddot{C}C(O)CH_3$ (open-shell treated by the half-electron method): Bachmann, C.: N'Guessan, T. Y., unpublished results.

(40) (a) Roth, H. D.; Manion, M. L. *J. Am. Chem. Soc.* **1976**, *98*, 3392–3393. (b) Lewars, E. G. *Chem. Rev.* **1983**, *83*, 519–534.

(41) Torres, M.; Ribo, J.; Clément, A.; Strausz, O. P. *Can. J. Chem.* **1983**, *61*, 996–998.

(42) Pople, J. A.; Raghavachari, K.; Frisch, M. J.; Binkley, J. S.; Schleyer, P. v. R. *J. Am. Chem. Soc.* **1983**, *105*, 6389–6398.

(43) Harding, L. B. *J. Am. Chem. Soc.* **1981**, *103*, 7469–7475.

(44) Dewar, M. J. S.; Kirschner, S. *J. Am. Chem. Soc.* **1971**, *93*, 4290–4294.

(45) (a) Davidon, W. C. *Comput. J.* **1968**, *10*, 406–410. (b) Fletcher, R. *Comput. J.* **1965**, *8*, 33–41. (c) Fletcher, R.; Powell, M. J. D. *Comput. J.* **1963**, *6*, 163–168.

(46) Cf. Scheme I, reaction B: $C_1C_2R_2$ angle for **2** and **3**; C_1R_2 for **4**. Reaction C: C_1CR''' for **2** and **4** ($R''' = H$) and for **3** ($R''' = CH_3$). Reactions D and E: C_1C_2O angle.

(47) (a) The use of the LD formula to ensure size consistency is questionable regarding the number n of electrons (n to 64 in **3**). Cremer and Thiel[47b] have reported LD and PSK[47c] corrections for systems with n to 90. They concluded that the PSK corrections provided better estimates of the correlation energy, particularly for high values of n, the differences from the LD corrections going to 9 kcal/mol. In the present calculations, the PSK corrections were also evaluated. However, the values thus obtained (relative energies and activation barriers) were identical with the corresponding LD values within 0.8 kcal/mol. This significant difference between our results and that of Cremer is possibly related to the size of the involved π systems (roughly 4π electrons in our systems, and $10\text{–}18\pi$ electrons in Cremer's work). Thus, one can expect that the inclusion of highly excited configurations in our systems is less important than in that studied by Cremer. It is also reflected by the C_0 values. C_0 being the coefficient of the SCF determinant in the normalized BWEN vector; throughout our calculations including those of transition states, the minimal C_0 value was 0.943, while in the results reported by Cremer and Thiel (concerning stable isomers only), the minimal C_0 value was ~0.913, indicating that correlation effects are more significant in their study. (b) Cremer, D.; Thiel, W. *J. Comput. Chem.* **1987**, *8*, 48–50. (c) Pople, J. A.; Seeger, R.; Krishnan, R. *Int. J. Quantum Chem. Symp.* **1977**, *11*, 149–163.

(48) Pedley, J. B.; Rylance, G. *Sussex-N.P.L. Computer Analysed Thermochemical Data: Organic and Organometallic Compounds*; Sussex University, Sussex, England, 1977.

(49) (a) Frisch, M. J.; Binkley, J. S.; Schlegel, H. B.; Raghavachari, K.; Melius, C. F.; Martin, R. L.; Stewart, J. J. P.; Bobrowicz, F. W.; Rohlfing, C. M.; Kahn, L. R.; Defrees, D. J.; Seeger, R.; Whiteside, R. A.; Fox, O. J.; Flender, E. M.; Pople, J. A. GAUSSIAN 86; Carnegie-Mellon Quantum Chemistry Publishing Unit: Pittsburgh, PA, 1984. (b) The open-shell systems were treated with the UHF formalism.[49c-e] (c) Berthier, G. *C.R. Acad. Sci. Paris* **1954**, *238*, 91–94. (d) Berthier, G. *J. Chim. Phys.* **1954**, *51*, 363–371. (e) Pople, J. A.; Nesbet, R. K. *J. Chem. Phys.* **1954**, *22*, 571–572.

Table V. MNDOC-SCF Geometries of Ketocarbenes (KC), Ketenes (KE) and Oxirenes (OX) of the 1-5 Series

		C-O[a]	C-C[a]	C-R_1[a]	C-R_2[a]	OCC[b]	CCR_1[b]	CCR_2[b]	R_1CCO[c]
KC[d]	1	1.209	1.476	1.104	1.124	129.1	108.5	109.3	96.3
	2	1.217	1.489	1.476	1.529	123.0	118.6	114.3	86.9
	3	1.218	1.490	1.510	1.573	119.8	125.8	118.4	73.1
	4	1.212	1.501	1.495	1.543	124.1	112.1	112.8	125.1
	5	1.212	1.536	1.445	1.515	120.1	112.7	119.6	180.0
KE	1	1.173	1.311	1.085		180.0	121.1		
	2	1.169	1.328	1.498		180.0	120.1		
	3	1.171	1.338	1.550		180.0	114.7		
	4	1.170	1.321	1.508		180.0	124.1		
OX[e]	1	1.425	1.296	1.070		62.9	162.8		180.0
	2	1.426	1.305	1.464		62.8	161.8		180.0
	3	1.426	1.307	1.495		62.7	161.9		180.0
	4[f]	1.426	1.306	1.465		62.7	131.9		179.7
	5[g]	1.398	1.407	1.340		59.8	126.4		180.0

[a] Bond lengths in angstroms. [b] Bond angles in degrees. [c] Dihedral angles in degrees. [d] R_1-C-C(O)-R_2. [e] In each oxirene, the two C-O bond lengths were held equal. [f] 7-Oxabicyclo[4.1.0]hept-1(6)-ene; half-chair conformation: C(2)-C(3) = 1.561 Å; C(3)-C(4) = 1.558 Å; C(1)C(2)C(3) = 103.3°; C(2)C(3)C(4) = 120.3°. [g] 7-Oxabicyclo[4.1.0]hept-1(6), 2,4-triene; C_{2v} symmetry being the result of calculation: C(2)-C(3) = 1.453 Å; C(3)-C(4) = 1.368 Å; C(1)C(2)C(3) = 109.9°; C(2)C(3)C(4) = 123.7°.

Discussion

In connection with **2**-OX identification,[16a] with the purpose to ascertain the ν(C=C) vibrational mode assignment to the 2137-cm^{-1} band,[50] we have performed ab initio calculations at the SCF level, using the 3-21G[51] and the 6-31G**[52] basis sets. We only report the calculated ν(C=C) vibrational frequencies between brackets: **1**-OX 3-21G (1944.6 cm^{-1}), 6-31G** (2001.8 cm^{-1}); **2**-OX 3-21G (2241.9 cm^{-1}). These results confirm that the presence of two methyl groups in **2**-OX strongly increases the ν(C=C) frequency (by ~300 cm^{-1}). Moreover, an additional increase is expected for **2**-OX when going to the 6-31G** basis set. It is known that, at this level of the theory, the vibrational frequencies are overestimated by ~10% on the average.[53] Thus, it appears that the above ν(C=C) assignment is satisfactory.

Before comparing the calculated activation barriers with experimental data, it is interesting to make some remarks about the relative energies (with respect to KE) and the structures of isomers, in particular KC[54] and OX species.

The relative energy of **2**-KC (60.7 kcal/mol) is similar to that of formylmethylene. The geometrical features of these two ketocarbenes are also close together. However, the relative energy of **4**-KC is slightly higher (66.3 kcal/mol) and the corresponding increase of 5.6 kcal/mol could partly result from ring strain. Indeed, upon going from **2**-KC to **4**-KC, the CC_1C_2 angle decreases from 118.6 to 112.1° and the C_1C_2C angle from 114.3 to 112.8°, while the CC_1C_2O dihedral increases from 86.9 to 125.1°.[55] In order to clarify the influence of the ring strain on the relative energy of **4**-KC, a supplementary calculation has been performed on **2**-KC with CC_1C_2 and C_1C_2C angles and CC_1C_2O dihedral fixed to the corresponding values of **4**-KC. Effectively, from this calculation an increase of 3.8 kcal/mol is obtained for the relative energy of this locked conformation.

The energy of **3**-KC is surprisingly lower (50.2 kcal/mol) since the geometrical deviations from **2**-KC (Table V) seem to be minor,

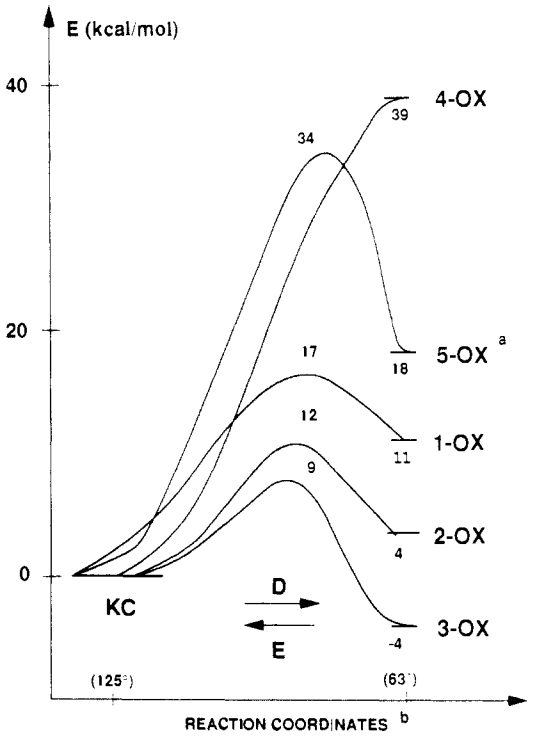

Figure 5. MNDOC-BWEN relative energies (in kilocalories per mole) with respect to KC for the D and E reaction paths. (a) **5**-OX: benzyne oxide. (b) C(1)C(2)O angle: see Table V.

(50) The vibrational spectra of **2**-OX and **2**-OX-d_6 have been identified on the basis of force field calculations,[16a] previously appraised owing to the good agreement between experimental and calculated vibrational frequencies of dimethylthiirene (thiooxirene). All the force constants, except F(C—S) and F(C=C), have been directly transferred to **2**-OX. To account for the **2**-OX experimental frequency assigned to the ν(C=C) vibrational mode (2137 cm^{-1}), we had to increase F(C=C) by 23%.

(51) Binkley, J. S.; Pople, J. A.; Hehre, W. J. *J. Am. Chem. Soc.* **1980**, *102*, 939-947.

(52) Hariharan, P. C.; Pople, J. A. *Theor. Chim. Acta* **1973**, *28*, 213-222.

(53) Hehre, W. J.; Radom, L.; Schleyer, P. v. R.; Pople, J. A. *Ab Initio Molecular Orbital Theory*; Wiley: New York, 1986.

(54) (a) The relative stabilities of the ketocarbenes, with respect to the corresponding ketenes, are overestimated through MNDOC-BWEN calculations.[61] But, it is expected that their stabilities relative to each other are correctly predicted. This assumption was supported by an additive MNDOC-BWEN calculation on a system with different R_1 and R_2 substituents. Indeed, ketocarbene **6**-KC (R_1 = CH_3, R_2 = C_6H_5) is destabilized by ~1.6 kcal/mol with respect to **7**-KC (R_1 = C_6H_5, R_2 = CH_3), suggesting that the percentage of oxirene participation from **7** is lower than that from **6**, in agreement with experimental results. From photolysis experiments on **6**-DZ and **7**-DZ, the oxirene participation was in the range 44-83% and 0-12%, respectively.[54b] (b) Regitz, M.; Rüter, J. *Chem. Ber.* **1969**, *102*, 3877-3890.

(55) It has been suggested that the CC_1C_2O dihedral values, usually close to 90°, allow some delocalization of the carbon lone pair into the carbonyl π system.[25] However, the singlet formylmethylene **1**-KC structure is questionable: Tanaka et al.[19] and Bouma et al.,[20] through their ab initio closed-shell calculations, obtained a HCCO dihedral value close to 90° (geometries optimized at the SCF level). Novoa et al.,[21] referring to the hypothesis of conformational control, concluded, from their MC-SCF calculations, that "the singlet ketocarbene is a planar biradical". In order to check the effect of electron correlation on the singlet **1**-KC structure within the MNDOC framework, we have optimized its geometry at the BWEN level. No significant deviation has resulted with respect to the SCF level optimization. In particular, the HCCO dihedral is again close to 90°. Moreover, the main configuration (closed shell) coefficient is relatively high (C_0 = 0.97), suggesting that the biradicaloid character is probably not predominant.

taking into account the relative flexibility of the carbenoid carbon atom. In **2**-KC and **3**-KC, the CC_1C_2 angle values are 118.6 and 125.8°, respectively, while the CC_1C_2O dihedral values are 86.9 and 73.1°, respectively. Note that these geometrical trends from **2**-KC to **3**-KC are related to the repelling *tert*-butyl substituents. In fact, the apparent stabilization of **3**-KC is a consequence of the biased reference with respect to which the relative energies are given in Table III. Indeed, in **3**-KE, the bulky substituents are so close to one another that three H–H inter-*tert*-butyl distances are less than 2.4 Å,[56] the shortest being 2.08 Å. Going from **3**-KE to **3**-KC allows a partial steric strain release, which is at the origin of the **3**-KC apparent stabilization. The same substituent effect easily explains the change in the $C_2C_1R_1$ angle that decreases from 120.1° in **2**-KE to 114.7° in **3**-KE, a somewhat important variation for an essentially sp^2 carbon atom.

Turning now to the oxirene species, the values reported in Table III and Figure 5 lead to the following remarks: **2**-OX is stabilized by 11.7 kcal/mol with respect to **1**-OX. As the geometrical parameters are rather similar (Table V), the stabilizing effect is possibly related to the σ-donating ability of the CH_3 substituents. On the other hand, **4**-OX is strongly destabilized (by ~40 kcal/mol with respect to **2**-OX), probably due to ring strain that prevents the CC_1C_2 angle from opening up to ~160°. In **4**-OX, this angle is limited to 131.9°. Actually, from the investigation of the reaction paths, it results that **4**-OX is not a stable intermediate, but on the contrary, a highly unstable transition state (Table IV and Figure 5). Effectively, from the results of photolysis experiments on **4**-DZ, Timm et al. have eliminated an oxirene participation.[57] Other similar studies also excluded oxirene participation.[9b,57b-e] Therefore, as the five- or six-membered ring cannot assumed a CC_1C_2 angle enlargement to ~160°, it seems impossible to isolate the corresponding oxirenes. This statement does not exclude the oxirene reaction path; actually, the oxirenes could be just transition states in these particular cases. Moreover, this statement does not mean that the corresponding ketocarbenes are also destabilized and that the only reaction paths are the concerted mechanism.[12] Nanosecond OX transients have been observed[58] during laser flash photolysis experiments on 1-oxo-2-diazo-1,2-dihydrobenzene (**5**-DZ) and related molecules; therefore, we have performed supplementary MNDOC-BWEN calculations on this system. Surprisingly, the corresponding oxirene (**5**-OX = benzyne oxide or 7-oxabicyclo[4.1.0]hepta-2,4,6-triene) lies in a relatively deep well, and it requires as much as 15 kcal/mol to isomerize (Figure 5), whereas the observed activation energy extends from 3 to 6 kcal/mol[58b] according to the solvent. Since the calculated CC_1C_2 angle is ~127°, it appears to contradict our previous assertion related to ring strain. However, the C_1C_2 bond length in **5**-OX (1.409 Å) is large compared to the typical oxirene C_1C_2 distance (1.306 Å; Table V); so **5**-OX looks intermediate between oxirene and oxirane (C–C = 1.500 Å).

The relative stabilization of **3**-OX partly results from the biased reference (see above). Therefore, it is more reliable to compare the oxirene energies when they are referred to the ketocarbene ones (Figure 5), since the intersubstituent interactions in ketocarbenes are expected to be consistently lower than in ketenes. If we compare the calculated activation energy for the **2**-*E* process (7.3 kcal/mol) with the experimental value (2 kcal/mol),[16a] we may emphasize the good qualitative agreement. Expecting, for a series, the parallelism between experimental and calculated data, we can predict that **3**-OX will be easily observed at low temperatures (Figure 5); moreover, the activation barrier order B ≈ C > D suggests that the D process would be largely favored in this case. In contrast, for **1** isomerization processes, it is clear that B will be faster than D (Table IV), which excludes any expectation to trap **1**-OX.

Before going further into Table IV, which reports the activation barrier values for different processes (B–E), we must remark that, during the first step A, the loss of the nitrogen molecule surely leads the ketocarbene to recover a large amount of vibrational energy. Indeed, the departure of the N_2 molecule is endothermic by ~30 kcal/mol,[59] while the wavelengths used in these experiments are currently in the range 230–458 nm, corresponding to photon energies greater than 60 kcal/mol. Moreover, from some deazotation experiments[60] it appears that, for the most part, the excess of vibrational energy (and rotational energy in gas phase) becomes localized on the carbon moiety rather than on the nitrogen molecule. Though RRKM simulations of B and C unimolecular processes would be possible, the following discussion is quite restricted to qualitative arguments. Indeed, the calculated values such as activation energies[61] and data related to the transition-state structures are not sufficiently accurate to perform valuable RRKM calculations, owing to the use of the reaction coordinate method. Moreover, the activation entropy effects have been neglected.

After **2**-DZ and **2**-DZ-d_6 photolysis in krypton matrix (Table II), the product yields show that the percent KE is always larger than percent ON; from the calculated energy barriers (Table IV), it can be predicted that the KE/ON ratio would be infinite. Performed in the gas phase[10] at low pressure, the **2**-DZ photolysis gave a KE/ON ratio larger than 4 and even larger than 50 when a buffer gas (argon) was introduced in the cell at 1 bar pressure (7 Torr **2**-DZ). That important variation suggested that reaction C only occurs from **2**-KC vibrational excited states. When the vibrational relaxation is allowed, i.e., the buffer gas deactivates **2**-KC, the KE/ON ratio is then in very good agreement with the forecast obtained from calculations. As the KE/ON ratios are very similar when the photolyses are performed in a krypton matrix or in a low-pressure gas phase, it is suggested that, in matrices, the vibrational relaxation rates are quite low. In fact, they depend on several factors,[62] the knowledge of which has to be improved for large molecules. A priori, a tunneling effect[63] could be also invoked for the hydrogen shift involved in reaction C. However, the KE/ON ratio from **2**-DZ-d_6 photolysis is not significantly different from the result of **2**-DZ photolysis. As these experiments have been performed at low temperature (12 K in a krypton matrix), it may be concluded that a tunneling effect is probably unimportant in this reaction.

Considering the reactions that follow the first step of **4**-DZ photolysis (Table IV), it is noticeable that the activation barrier of reaction B, a ring contraction, is lower than the corresponding values for CH_3 and $(CH_3)_3C$ migrations occurring on **2**-KC and **3**-KC, respectively. It may be related to the fact that **4**-KC is the less stable ketocarbene among the three under investigation (Table III). Moreover, reaction C of **4**-KC presents an activation barrier that exceeds by ~9 kcal/mol that of reaction B (Table IV), in good agreement with the experimental KE/ON ratio (>20) observed when **4**-DZ has been photolyzed in the gas phase[10] or in solution.[5]

Several experiments on the photolysis of **3**-DZ showed that the KE/ON ratio is rather sensitive to experimental conditions: in

(56) The sum of the van der Waals radii according to: Bondi, A. *J. Phys. Chem.* **1964**, *68*, 441–451.

(57) (a) Timm, U.; Zeller, K. P.; Meier, H. *Tetrahedron* **1977**, *33*, 453–455. (b) Majerski, Z.; Redvanly, C. S. *J. Chem. Soc., Chem. Commun.* **1972**, 694–695. (c) Zeller, K. P. *Z. Naturforsch., B: Anorg. Chem. Org. Chem.* **1976**, *31B*, 586–588. (d) Zeller, K. P. *J. Chem. Soc., Chem. Commun.* **1975**, 317–318. (e) Zeller, K. P. *Chem. Ber.* **1975**, *108*, 3566–3573.

(58) (a) Tanigaki, K.; Ebbesen, T. W. *J. Am. Chem. Soc.* **1987**, *109*, 5883–5884. (b) Tanigaki, K.; Ebbesen, T. W. *J. Phys. Chem.* **1989**, *93*, 4531–4536.

(59) A value of 22.7 kcal/mol from an independent MNDOC-BWEN calculation on **2**-DZ, assuming the diazoketone, the ketocarbene, and the N_2 molecule to be in their ground singlet state; 35 kcal/mol from an EHT calculation[17] on the same α-diazoketone; 30 kcal/mol from an ab initio calculation on **1**-DZ.[19]

(60) (a) Chang, M. H.; Jain, R.; Dougherty, D. A. *J. Am. Chem. Soc.* **1984**, *106*, 4211–4217. (b) Holt, P. L.; McCurdy, K. E.; Adams, J. S.; Burton, K. A.; Weisman, R. B.; Engel, P. S. *J. Am. Chem. Soc.* **1985**, *107*, 2180–2182. (c) Adams, J. S.; Burton, K. A.; Andrews, B. K.; Weisman, R. B.; Engel, P. S. *J. Am. Chem. Soc.* **1986**, *108*, 7935–7938.

(61) The ketocarbene stability is probably overestimated by MNDOC[22] since, for the **1** system, its relative energy with respect to ketene is lower than the reference value of Tanaka et al.[19] by about 18 kcal/mol. However, this failure does not prevent from qualitative comparisons of activation energies of reactions evolving from the same ketocarbene.

(62) Bondybey, V. E.; English, J. H. *J. Chem. Phys.* **1980**, *73*, 87–92.

(63) Bell, R. P. *The Tunnel Effect in Chemistry*; Chapman and Hall: New York, 1980.

solution (CCl_4, THF)[10,12] or in argon matrix,[41] this ratio was very low with **3**-ON yields being larger than 95%; in the gas phase,[10] we observed the formation of 38% KE, which brought out an argument against the concerted mechanism hypothesis. This last observed competition is in good agreement with the calculated B and C activation barriers, which are very close to each other (Table IV). The methyl shift leading to **3**-ON has an activation barrier (24.6 kcal/mol) close to that one calculated for the hydrogen shift occurring during the **2**-KC → **2**-ON process (23.0 kcal/mol). Expecting a larger difference, we may emphasize the relief of steric hindrance in the **3**-KC *tert*-butyl group.[64] In addition, it is interesting to note that the WR activation barrier related to the CH_3 shift (**2**-KC → **2**-KE, 12.7 kcal/mol) is larger than the corresponding value of **1** (2.4 kcal/mol) by ~10 kcal/mol. This comparison is probably reliable since the latter value (2.4 kcal/mol) is in agreement with the reference ab initio value of Tanaka et al. (0.0 kcal/mol).[19] Similarly, it is noticeable that the WR activation barrier related to the *tert*-butyl shift (23.3 kcal/mol) is greater than the CH_3 shift value by ~10 kcal/mol. This increase could originate from steric hindrance occurring in the transition state of **3**-KC → **3**-KE. Its structure presents a 131° dihedral angle ($R_1C_1C_2R_2$), a value to be compared with that (105°) of the **2**-KC → **2**-KE transition state.

The most important features of photolysis experiments reported in this paper, and those of previous experiments performed in the gas phase, form, with several hypotheses from the literature, an intricate puzzle; it seems a difficult task to bring them together in a consistent set. Nevertheless, using several experimental data and energy differences from our MNDOC-BWEN calculations and from some ab initio ones, we have been able to establish a full energy diagram (Figure 6), approximately scaled for the different **2** species (see notes in Figure 6). This diagram, and further comments, will be used as a conclusion. The commentaries will be focused on the ability of the diagram to account for the main observed processes.

First, we must emphasize that the photolysis and photoisomerization processes only occur on the singlet PES; arguments have been presented to support this hypotheses. As we have detected $KC(T_0)$ among the reaction products isolated at low temperature, the diagram must underline the occurrence of intersystem crossing between the ketocarbene singlet and triplet states. Therefore, the ultimate step of DZ photolysis requires, in order to isomerize $KC(T_0)$, a broad-band irradiation, which extends to visible (Table II; irradiation at $\lambda > 230$ nm); it would be

$$KC(T_0) + h\nu \text{ (visible)} \rightarrow KC(T_1) \rightarrow KC(S_1) \rightarrow KE + ON$$

Owing to the selectivity variation (increasing KE/ON ratio) when the irradiation changes from monochromatic (457.9 nm) to broad band ($\lambda > 230$ nm) (Table II), we suggest that, in the latter case, photolysis occurs, for a large part, directly from $DZ(S_n)$ giving $KC(S_n)$, which would evolve selectivity to KE. The $DZ(S_n \rightarrow S_1)$ process and the vibrational relaxations $S_0(v) \rightarrow S_0(v = 0)$ would be slower than generally assumed in condensed media.

The second step involves a competition between three reaction paths; the WR (path B) occurs from $KC(S_1)$ in its lowest vibrational level, whereas the concurrent reaction (path C) results from excited vibrational levels. The last $KC(S_1) \rightarrow$ OX reaction path requires activation energies (Table IV) that allow, for **2**-KC isomerizations, a balanced competition with the WR reaction; but **3**-KC → **3**-OX looks much faster than **3**-KC → **3**-KE. Therefore, it is suggested that, for some structures, OX may be a necessary reaction intermediate; then we must consider its evolution toward products that are stable at room temperature. It is noticeable that the 457.9-nm irradiation does not isomerize **2**-OX (Table III), which implies that its S_1 excited state is higher than S_0 by more than ~63 kcal/mol. From an UHF-3-21G calculation, the adiabatic $S_1 \leftarrow S_0$ transition energy is estimated to 63 kcal/mol for **1**-OX, in agreement with the value (68 kcal/mol) proposed by Tanaka et al.[19] Since the spin contamination is important in this S_1 calculation ($S^2 = 1.037$), it may be forecast that this calculation overstabilizes S_1; consequently, the real $S_1 \leftarrow S_0$ transition energy is certainly larger than 63 kcal/mol; consequently, the corresponding absorption wavelength is surely less than 460 nm. Moreover, the adiabatic $S_1 \leftarrow S_0$ transition energy has been estimated for **2**-OX through an UHF calculation that provides a larger value (73 kcal/mol; $S^2 = 1.037$). Hence, the selective OX → KE photoisomerization requires shorter wavelengths, as observed during **2**-DZ-d_6 photolysis (Table II). It is noticeable that the diagram scaling locates, just at the same energy level, $DZ(S_n)$ and $OX(S_1)$; thus, we postulate that they give the same $KC(S_n)$ state, which evolves mainly toward KE.

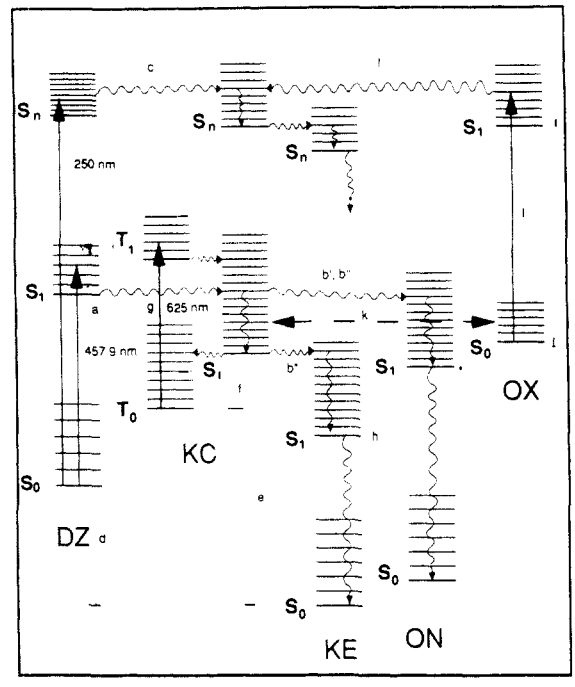

Figure 6. Energy diagram for absorption, photoisomerization, and vibrational relaxation processes involved in α-diazoketone photolysis. (a) DZ: $S_1(v = 0) - S_0(v = 0) \approx 60$ kcal/mol corresponding to the highest wavelength of the visible part of α-diazoketone electronic spectra. (b) Experiments on **2**-DZ irradiated at $\lambda = 457.9$ nm: (b') in gas phase at low pressure (7 Torr) preventing fast vibrational relaxations (**2**-ON yield 22–28%);[10] (b'') in gas phase at 1 bar pressure (argon) promoting fast vibrational relaxations (**2**-ON yield <5%);[10] (b''') in krypton matrix (**2**-ON yield 30–50%; this study). (c) Experiment on **2**-DZ isolated (1/2000) in krypton matrix and irradiated at $\lambda > 230$ nm (**2**-ON yield < 20%; see Table II). (d) MNDOC-BWEN calculations on **2**-DZ and **2**-KE: ΔH_f (kcal/mol) = 15 (DZ), −30 (KE), and 8 (N_2). (e) MNDOC-BWEN calculations on **2**-$KC(S_1)$: ΔH_f = 30 kcal/mol; $\Delta\Delta H_f$(KC − KE) corrected by 18 kcal/mol owing to overstabilization of KC.[61] (f) Ab initio calculations on **1**-KC ($S_1 - T_0$) (17 kcal/mol) and **1**-OX ($S_1 - S_0$) (68 kcal/mol).[19] (g) λ_{max} for KC issued from 2-diazoacenaphthenone photolysis.[9] (h) **1**-KE: $\lambda \leq 473$ nm.[65] (i) **2**-ON: $\lambda \leq 365$ nm. (j) MNDOC-BWEN calculations: **2**-$OX(S_0)$ − **2**-$KC(S_1)$ $\Delta\Delta H_f \approx 4$ kcal/mol. (k) Experiments in xenon matrix at 10 K: **2**-KC-(S_1, $v \neq 0$) → **2**-OX, and at 25 K **2**-OX → **2**-KC → **2**-KE.[16] (l) **2**-$OX(S_0)$ $h\nu$→ **2**-$OX(S_1)$ → **2**-$KC(S_n)$ → **2**-KE.

Experimental Section

Matrix Isolation Experiments. The apparatus and experimental technique have been already described.[16b] The relative concentrations of rare gas and DZ room-temperature mixture (M/S ratio) have been adjusted through pressure measurements; reproducible solute partial pressures required the use of a Datametrics (Barocel, series 600) capacitive manometer. The deposition rates of gas mixtures have been controlled with an Air Liquide microleak (VIP/RX); it never exceeded 2 mmol/h.

(64) In order to estimate this effect, a further calculation has been performed on a process

$$CH_3CH_2\ddot{C}C(O)CH_3 \rightarrow CH_2{=}C(CH_3)C(O)CH_3$$

that simulates the methyl shift with reduced steric hindrance. Indeed, the calculated activation barrier (29.3 kcal/mol) exceeds by 4.7 kcal/mol the corresponding value for **3**-KC → **3**-ON. Accordingly, it is expected that this excess represents to some extent the destabilization of **3**-KC resulting from the steric strain in the *tert*-butyl group.

(65) Laufer, A. H.; Keller, R. A. *J. Am. Chem. Soc.* **1971**, *93*, 61–63.

FT-IR Spectroscopy. The IR spectra were recorded on a 7199 Nicolet spectrometer. The resolution was 0.12 cm^{-1} without apodization. Owing to multiscan procedure, signal/noise ratios were at least larger than 50, even in the worse cases. The integrated intensities A (cm^{-1}) were measured as the area between the spectrum and the absorbance base line that joined the absorption band wings.

Irradiation Techniques. The broad-band (230–900 nm) irradiations were carried on by an Osram 200-W high-pressure mercury lamp equiped with a quartz envelope. The cryostat KBr windows filtered the beam at $\lambda > 230$ nm. The monochromatic irradiations were performed with an ionized argon laser working at 457.9 nm, the maximum power being 250 mW.

Kinetic Analysis. To fit the experimental integrated intensities at different times to exponential behaviors (decay of DZ or increase of KE, ON, or OX absorption bands), least-squares analysis were performed using a program that provides the first-order rate constants and the calculated integrated intensity values at zero and infinite time and their standard deviations. These are collected in Table I. For the two first kinetics, the rate constant inaccuracies do not exceed 5% for the DZ decay and 10–15% for the reaction product rises, the highest inaccuracies occurring when A_∞ is less than 0.05 cm^{-1}. As we observed that $k(DZ) > k(KE) \approx k(ON) \approx k(OX)$, we had to exclude simple kinetic schemes such as competitive reaction paths directly issued from DZ. Thus, we considered the occurrence of a reaction intermediate [DZ–(k)→X], from which were formed the different reaction products [X–(k_i)→P_i]; but we must eliminate the hypothesis of large rate constant differences ($k \gg k_i$) between the two steps. To check the validity of our approximate treatment of product rise kinetics, we simulated them through the following kinetic equation:

$$[P_i] = [DZ]_0 \frac{k_i}{\sum_j k_j - k}\left[(1 - \exp(-kt)) - \frac{k}{\sum_j k_j}(1 - \exp(-\sum_j k_j t))\right]$$

For different postulated $\sum k_j/k$ ratio ranging from 0.7 to 1.05, we calculated P_i value sets; each one was analyzed as resulting from a first-order process; the differences between the calculated and initially postulated k_i values never exceeded 10%. The observation of a large difference between k_i values of 2-ON-s-Z in α and β sites (Table I) underlined how fallacious would be a more sophisticated kinetic treatment when we were unable to discriminate between the absorption bands belonging to molecules isolated in different sites. In comparison with the other rate constants, those of OX molecules are too large to account for estimated OX yields never exceeding 9% (Table II); we may suggest that the observed OX absorption bands just correspond to one site, the other ones being hidden by the very close KE absorption bands.

Product Yields. For matrices having the same M/S ratio, when their thickness (l) have been carefully measured, it was possible to estimate, for each absorption band, relative integrated absorbance coefficients ϵ' defined, from the Beer–Lambert law, as $\epsilon' = \epsilon c = A/(xl)$, x being the molar fraction of the corresponding species belonging to a conformational or a product mixture.

Pure 2-ON has been isolated in a krypton matrix (M/S = 2000; l = 0.0145 cm) and photoisomerized (s-E to s-Z; $\lambda > 230$ nm). Integrated absorbances (A in cm^{-1}) at different irradiation times (0, 2, and 18 h) were measured: 0.4545, 0.5361, 0.7228 (s-Z 1730–1700 cm^{-1}), 1.069, 0.9285, 0.5780 (s-E, 1700–1670 cm^{-1}). From these values, we easily calculated the different unknowns: relative coefficients ϵ' (cm^{-2}) 72.5 (s-Z), 130.3 (s-E); molar fractions at the different times, x(s-Z) 0.43, 0.50, 0.694.

2-DZ-d_6 has been isolated in a krypton matrix (M/S = 2000; l = 0.0148 cm). After complete photolysis (49 min), first annealing, extended irradiation (1100 mn) of the reaction mixture at $\lambda > 230$ nm (see Table II) and final annealing (25 K; 20 mn), the integrated absorbances (A in cm^{-1}) were 1.267 (2-KE-D6 2130–2104 cm^{-1}), 0.167 (2-ON-d_6-s-Z 1730–1700 cm^{-1}), and 0.058 (2-ON-d_6-s-E 1700–1670 cm^{-1}). From the last two values, we estimated the 2-ON-d_6 conformer molar fractions (0.155 and 0.030, respectively). Observing complete thermal isomerization of 2-OX-d_6 (last annealing) and total photoisomerization of 2-KC-d_6 being assumed, 2-KE-d_6 was the last product to be considered; obviously, its molar fraction was calculated as 1 – (0.155 + 0.030) = 0.815. Therefore, the ϵ' coefficient of its ν(C=C=O) absorption band was estimated at 105.04 cm^{-2}.

When the same matrix has been annealed for the first time, the 2-OX-d_6 absorption spectrum vanished ($\sum A$ = –0.101 cm^{-1}; 2135–2130 cm^{-1}), whereas 2-KE-d_6 integrated absorbance increased ($\sum A$ = +0.108 cm^{-1}; 2130–2104 cm^{-1}). 2-ON-d_6 integrated absorbances being unchanged, the 2-OX-d_6 ϵ' coefficient was estimated to be 98±2 cm^{-2}.

Ketocarbene 2-KC-d_6(T_0): Vibrational Absorption Bands. During the photolysis of 2-DZ-d_6 (krypton matrix, λ = 457.9 nm, T_D = 12 K; Table II), we observed some absorption bands (758, 1028, 1032, and 1096 cm^{-1}) that have low integrated intensities ($A \leq 0.013$ cm^{-1}). They may be attributed to 2-KC-d_6(T_0). From the integrated absorbance values measured at 420 and 1110 min, the $A(420)/A(1110)$ ratios have been checked to be constant: 1.7 (757–761 cm^{-1}), 1.8 (1025–1034 cm^{-1}), and 1.7 (1093–1100 cm^{-1}). When the irradiation was performed at $\lambda > 230$ nm (Table II), the same absorption bands increased until 25 min; a subsequent fast decrease was observed between 25 and 49 min and the bands completely vanished at 1110 min. It may be noticed that the ketocarbene issued from 2-diazoacenaphthenone photolysis has been characterized[9a] by three IR frequencies at 767, 1015, and 1665 cm^{-1}. This last value has been associated to ν(C=O). With a saturated substrate such as 2-KC, we expected an absorption at higher frequency. The first observed absorption band (1707–1702 cm^{-1}) that fit this requirement was previously assigned to 2-ON-d_6-s$Z\beta$ (Table I). As an exceptional high rate constant was associated with this band, we assumed that the 2-ON-d_6-s$Z\beta$ and 2-KC-d_6 absorption bands superimposed. The next hypothesis was the equality of integrated absorption coefficients of s$Z\beta$ and s$Z\alpha$ molecules and the same kinetic behavior; then, it was possible to assess[16b] the relative integrated absorption coefficient of 2-KC-d_6(T_0) to be $\epsilon' \approx 10$ cm^{-2}. This value is surely very approximate but it may be justified owing to the large delocalization that can occur in an acyclic KC(T_0) species[9a] and therefore reduce the ν(C=O) ϵ' coefficient.

Acknowledgment. This research was supported by grants from the Centre National de la Recherche Scientifique (ATP dynamique réactionnelle des systèmes simples) and from the Ministère de la Coopération et du Développement (Paris). Funds to purchase the FT-IR spectrometer have been provided by the Mission de la Recherche and the Conseil Régional Provence-Alpes-Côte d'Azur. Calculations were performed on IBM 4341 Computers at Office Central de Mécanographie (Abidjan). For helpful discussions, Professors F. D. Greene and Gh. D. Mateescu are gratefully acknowledged.